Effect of low content sintering aids addition on β-SiC sintered by spark plasma sintering

Florimond Delobel, J Cambedouzou, Florence Moitrier, Sébastien Lemonnier

Version of Record: https://www.sciencedirect.com/science/article/pii/S0955221922000504
Manuscript_45b3399aa728a65c53acfe3d8b256311

Effect of low content sintering aids addition on β-SiC sintered by Spark Plasma Sintering

Florimond Delobel [a, b, *], Julien Cambedouzou [b, c], Florence Moitrier [a], Sébastien Lemonnier [a, *]

[a] French-German Research Institute of Saint-Louis, Saint-Louis, France
[b] ICSM, CEA, CNRS, ENSCM, Univ Montpellier, Marcoule, France
[c] IEM, CNRS, ENSCM, Univ Montpellier, Montpellier, France
* Corresponding authors: f.delobel@bcrc.be, sebastien.lemonnier@isl.eu

Abstract

The influence of low content of sintering aids addition on the properties of β-SiC sintered by spark plasma sintering was studied based on X-ray diffraction and SEM observations. Three dopants, respectively Al_2O_3, Al_2O_3-Y_2O_3 and Al_2O_3-AlN were chosen, and the investigation was undertaken in the [0.5wt.% - 5wt.%] content range. The analyses revealed the possibility to increase the density of sintered pellets close to 100% of theoretical density (T.D.), even with the addition of very low sintering aids contents, as low as 0.5wt.%, for each dopant. The combination with high sintering pressure allowed keeping a fine microstructure and a pristine cubic crystalline structure while avoiding the formation of secondary phases.

Keywords: Silicon Carbide, Spark Plasma Sintering, sintering aids

1 Introduction

Silicon carbide (SiC) attracts considerable attention in the field of materials research due to its exceptional mechanical, thermal and electronic properties [1]. Thanks to its high hardness and low density, this ceramic material presents a great interest for ballistic protection, especially in dual hardness armour [2], [3]. Indeed, these properties make it as competitive as other carbides against small-calibre projectile or Armor-Piercing Fin Stabilized Discarding while presenting much lower cost [2]. Moreover, Chen et al. demonstrated an amorphization phenomenon for boron carbide against heavy core projectile, as tungsten carbide, which leads to a drastic increase of the brittle behaviour of the ceramic and thus a substantial

decrease of ballistic performances. On its side, SiC does not encounter such a transition and finally demonstrates a higher efficiency if this kind of projectile has to be considered [4].

SiC ceramics developed for ballistic applications are never composed of pure β-SiC while the cubic form of SiC was reported to exhibit isotropic properties and better hardness than the hexagonal structure [5]. This is due to densification limitations induced by a limitation of sintering temperature. Indeed, the covalent character of SiC chemical bonds makes its sintering very difficult [1] and full density was only reported at very high temperature and/or with sintering aids [6]–[8]. The sintering of SiC at very high temperature (>1900°C) leads to higher final density but induces the phase transition into hexagonal polytypes. On the other side, the use of sintering aids leads to the presence of secondary phases, which could be detrimental for mechanical properties due to their lower hardness than pristine SiC. The development of dense and cubic SiC exhibiting isotropic properties and high hardness is thus a promising approach for the improvement of ballistic performances. Recent studies concerning the modification of the sintering behaviour of a pure and cubic SiC nano-powder were reported [9]. Lemonnier et al. mixed two different grades of nanopowders with different particle sizes and showed that better rearrangement ability and higher final density were possible thanks to a modification of the rheological behaviour of the starting powders attributed to both the mixing steps and the wider range of particle size. Full density was reached without sintering additives for sintering temperature of 2100°C under 80 MPa but grain growth and α-SiC were observed [9]. In order to get denser SiC of pure cubic SiC, we set up an approach combining the application of high-pressure during sintering and the use of very low sintering aid amount. Indeed, in a recent study, we investigated the role of sintering pressure on the cubic into hexagonal phase transition [10]. We showed the possibility to stabilize the cubic form of SiC at higher temperature than 1900°C by applying high sintering pressure while increasing the density of SiC pellets until 95% of T.D.. By this way, only few percent of density have to be gained and thus it can be expected that a very low fraction of sintering aid, in comparison with the literature, could be enough to achieve full density while maintaining the cubic structure.

In this work we investigated the low content addition effect of different sintering aids (Al_2O_3, Al_2O_3-Y_2O_3 and Al_2O_3-AlN) on the sintering behaviour and crystalline phase composition of SiC ceramics. The choice of these three sintering aids, generally added with a content of about 5wt.% to 15wt.%, was based on their capacity to widely increase the densification of SiC materials by improving particles rearrangement thanks to the apparition of a liquid phase during sintering [11]. Indeed, it is well known in the literature that the Al_2O_3 compound reacts with silica at the surface of SiC particles in order to form an eutectic above 1600°C and to favour dissolution-precipitation mechanisms [6], [12], [13]. Other studies demonstrated that

the Al_2O_3-Y_2O_3 compound will rather form this eutectic from 1816°C [14]–[17]. This mixture is generally known to modify the microstructure of SiC by both apparition of elongated grains and secondary phases like YAG compound [18], [19]. However, even if the presence of elongated grains could improve tenacity properties of the material [20], [21], the preferred fine microstructure consisting of equiaxed grains required for high hardness and ballistic performances [10], [22] should be obtained by combining very low dopant content addition and application of high sintering pressure. Finally, the AlN compound, mixed with alumina, is most often used to stabilize the cubic phase thanks to its high viscosity. Indeed, it is known to shift the phase transition temperature of SiC by inclusion of nitrogen element in the crystalline lattice that limits the mass transport mechanisms. This compound also allows keeping a microstructure with equiaxed grains by inhibition of grain growth [17], [23]–[25]. In addition to density determination, the obtained doped samples will be characterized by means of X-ray diffraction analyses and SEM observations, and compared with undoped samples to determine the role of sintering aids addition on the evolution of microstructure and crystalline structure of silicon carbide.

2 Experimental

2.1 Materials

The pristine SiC powder is a high purity (99.999%) commercial β-SiC powder produced by laser pyrolysis, with an average grain size of 35nm, which was purchased from Nanomakers (France) and called NMK in the following.

Three sintering aids were chosen to be mixed with the SiC powder: high purity monoclinic α-Al_2O_3 (99.9%) with a grain size lower than 1µm (Alfa Aesar), high purity cubic Y_2O_3 (99.995%) with an average grain size of 50-70nm (Alfa Aesar), and high purity AlN (> 99%) with a grain size lower than 100nm (Sigma Aldrich). The α-Al_2O_3 was added alone to SiC powder while the Y_2O_3 and AlN aids were mixed with α-Al_2O_3 before addition, respectively with a 63wt.%-37wt.% proportion for the α-Al_2O_3-Y_2O_3 mixture (corresponding to YAG[1] stoichiometric composition) and a 50wt.%-50wt.% proportion for the α-Al_2O_3-AlN mixture.

Each “SiC powder + sintering aid” mixture was performed in a 3D powder blender mixer (Turbula ®) during 1hour at a speed of 49rpm using a total powder mass of 10g. Two weight

[1] YAG: Yttrium Aluminium Garnet

contents of sintering aids were experimented: 5wt.% and 0.5wt.%. The Table 1 reports the used sintering aid mass and the corresponding mixture name.

Table 1 - Summarized table of the sintering aids mixtures: added dopant, name of the mixture and its composition.

Sintering aid	Mixture name	Weight content (wt%)	SiC powder mass (g)	Aid powder mass (g)
α-Al_2O_3	A500	5	9.50	0.50
	A50	0.5	9.95	0.05
α-Al_2O_3-Y_2O_3	AY500	5	9.50	0.50
	AY50	0.5	9.95	0.05
α-Al_2O_3-AlN	NA500	5	9.50	0.50
	NA50	0.5	9.95	0.05

2.2 Sintering parameters

Spark Plasma Sintering (SPS) was performed to consolidate powders using a SPS HP D125 apparatus from FCT Systeme GmbH. The SiC powders were introduced in a graphite die with an inner diameter of 30mm. Three layers of graphite felt with a thickness of 6mm were wrapped around the graphite die and two other layers were put over and under it to limit thermal losses during sintering. A cold pre-compaction at 100kg/cm² was applied to keep the system in. Then, the latter was heated using DC pulse current. An optical pyrometer was used to control temperature at a distance of 3mm from the sample through a hole in the upper puncher, this configuration ensuring a reliable measurement of sample temperature.

Samples were sintered with a temperature of 2000°C using a heating rate of 10°C/min under vacuum atmosphere. Various sintering pressures from 17 to 127MPa were applied and a dwell of 10min at maximum temperature was set. The pressure was released at the end of the dwell time and the cooling step was not controlled. Note that the temperature of 2000°C was chosen in order to ensure a high densification of SiC samples (> 90% for undoped samples [10]) while limiting severe creep deformation of graphite tools.

2.3 Physical and chemical characterizations

A D8 Advance Bruker AXS instrument (Cu Kα radiation, λ = 0.154 nm) was used for X-ray diffraction analyses. Microstructural observations were performed using a Nova NanoSEM^{TM} 450 from FEI company scanning electron microscope. The densities of sintered samples were measured by the Archimede's method and confirmed by geometrical measurements.

Grain sizes measurements were performed thanks to *ImageJ* software and the given values, as well as the standard deviation values, were obtained by average of the measurement of 50 grains.

3 Results and discussion

3.1 Standard sintering aid content

A first series of sintering experiments was performed on SiC powders with a doping amount of 5wt.% Al_2O_3, Al_2O_3-Y_2O_3 and Al_2O_3-AlN to highlight potential reaction and estimate the efficiency of additives on the NMK powder densification. These tests were carried out under a sintering pressure of 17MPa to let degassing any potential gas during heating. Indeed, some authors reported in the literature that the addition of alumina could sometimes create some gaseous species, leading to residual porosity, during its reaction with the silica at the surface of SiC particles [6], [12], [13].

Figure 1 presents SPS curves of the three samples sintered from the additive-bearing powders mixtures compared to the “reference 17MPa” sample – i.e., the raw SiC powder in the as-received condition - and the “NMK-no sintering aids” sample – i.e., the raw powder which was blended during 1hour without addition of sintering aids. The latter sample was considered to evaluate any potential effect of blending on the densification behaviour of SiC powder.

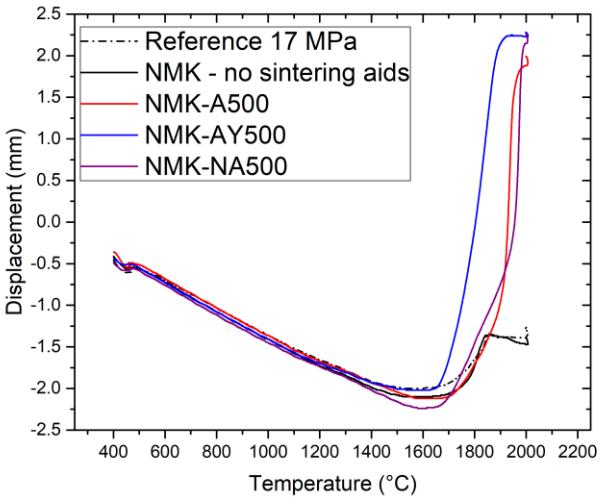

Figure 1 - Sintering behaviour curves of samples sintered with the Al_2O_3, Al_2O_3-Y_2O_3 and Al_2O_3-AlN mixtures with 5wt.% of sintering aids compared with the reference 17MPa and NMK-no sintering aids samples.

Figure 1 shows similar dilatation step for each sintered powder from room temperature until 1400°C. For both powders sintered without sintering aids, similar behaviours are clearly visible with only a limited shrinkage in the range [1400°C - 2000°C]. On the opposite, an important shrinkage and high sintering kinetic can be observed for the three samples with additives. Thus, even if the addition of sintering aids slightly delays the temperature of sintering beginning, appearing at 1520°C for raw powders versus 1540°C, 1570°C and 1580°C respectively for the AY500, A500 and NA500 mixtures, the important displacement suggests much higher final densities.

Note that the presence of AY500 mixture induces a higher sintering kinetic than A500 and NA500 mixtures. Indeed, the slope of the curve is much higher than the other ones. Moreover, this curve also presents a knee during the sintering step at lower temperature (≈ 1650°C) compared to the curves of the NMK-A500 and NMK-NA500 samples (respectively ≈ 1700°C and ≈ 1680°C). This observation lets suppose a higher efficiency of the AY500 mixture addition regarding particles rearrangement during sintering.

The Table 2 reports density values measured for these 5 samples. For the calculation of the relative density, the exact composition of each ceramic was considered. The results confirm the observations deduced from the SPS curves. Indeed, both samples sintered without sintering aids have a density of about 50% of T.D., while the three other samples reach values of 98-99% of T.D. These high densities are even reached with alumina addition even

though the sintering curves indicate a slightly lower shrinkage compared to the two others. This may be explained by a denser green body obtained after the cold pre-compaction (experimentally measured at 1.18g/cm³ for the NMK-A500 sample against 1.02 and 0.99g/cm³ for the NMK-AY500 and NMK-NA500 samples, respectively). Moreover, these values seem to indicate that in our case alumina addition does not lead to gaseous species formation, as occasionally described in the literature, by reaction with silica at the surface of SiC particles that could limit the material densification (porosity formation) [6], [12], [13]. This is consistent with the constant level of vacuum measured all along the sintering experiment in the SPS chamber. The absence of gaseous species formation could be explained by a very low content of silica in our high purity SiC powder and/or a low alumina amount which are not favourable for this formation.

Note that the NMK-AY500 sample presents a similar density than the two other doped samples despite of its different sintering behaviour noticed in the sintering curve.

Table 2 –Table summarizing the SiC pellets densities after sintering at 2000°C under 17 MPa

Sample	Density (% of T.D.)
Reference 17MPa	50 ± 1%
NMK-no sintering aids	52 ± 1%
NMK-A500	99 ± 1%
NMK-AY500	99 ± 1%
NMK-NA500	98 ± 1%

X-Ray diffraction analyses were performed on the five samples. The experimental XRD patterns are presented in Figure 2. Note that the experimental pattern of the sample “Reference 17MPa” is not presented here because it is completely superposable to the one of the sample “NMK-no sintering aids”. For all the samples, cubic phase (JCPDS card 03-065-0360) is not the only SiC polytype in presence. Indeed, the high temperatures reached (2000°C), combined with the low SPS pressure (17 MPa), make the cubic to hexagonal transition possible as demonstrated in a previous study [10]. It is possible to notice the presence of the 6H polytype (JCPDS card 00-029-1131) at 2θ = 34.2° ((101) atomic plane) for all the samples. Nevertheless, only the free-additive sintered samples and the one mixed with the NMK-NA500 mixture show the (103) atomic plane diffraction peak, identified at 2θ = 38.2°. This could be explained by a 3C-6H transition not sufficiently complete in the two other samples (i.e.: NMK-A500 and NMK-AY500). Another Bragg peak, identified at 2θ = 34.4°,

appears in the patterns of samples NMK-A500, NMK-AY500 and NMK-no sintering aids. This peak could correspond in an intermediate state of the polytypic transition, particularly to a rhombohedral polytype.

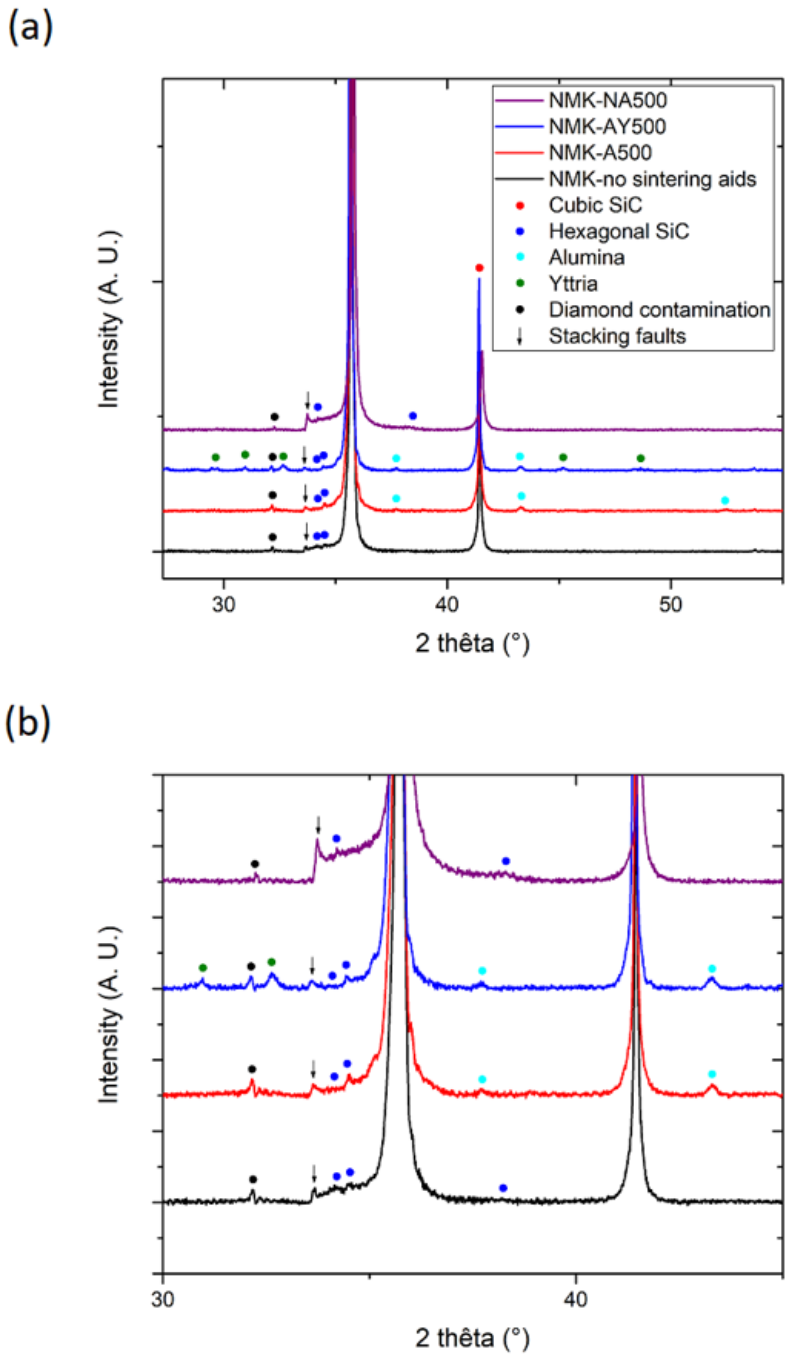

Figure 2 - Experimental XRD patterns of samples sintered with the Al_2O_3, Al_2O_3-Y_2O_3 and Al_2O_3-AlN mixtures with 5wt.% of sintering aids compared with the one of raw NMK. The figure (a) represents the [27°-55°] scattering angles range and the figure (b) represents a zoom in the SiC peaks range.

In addition to SiC peaks, it is possible to notice other peaks, which correspond to sintering aids. The four XRD patterns show the presence of diamond (JCPDS card 01-089-8493) due to residual crystals in the porosity after polishing (identified peak at 2θ = 32°). The patterns of the two samples NMK-A500 and NMK-AY500 show several peaks, which can be attributed to the sintering aids, particularly alumina (JCPDS card 01-075-0921) and yttria (JCPDS card 01-089-5592). Finally, in the case of NMK-NA500 sample, the presence of beta and alpha SiC polytypes indicate that transition occurred even if the literature seemed to indicate the opposite. This could be explained by sintering conditions, which favour the polytypic transition preferentially to the stabilization of cubic phase due to too smaller content of sintering aids (5wt.%, and thus 2.5wt.% of AlN) compared to the one generally reported in the literature (from 5 to 15wt.% [6], [12], [13], [15]–[17], [20], [23]–[25]). In addition, the fact that the sintering aids (Al_2O_3-AlN) are no more visible do not attest to the absence of secondary phase (resulting from the addition of sintering aid), but could mean either a content lower than the detection threshold of XRD apparatus or the formation of amorphous phases (under the form of residual liquid phases).

3.2 Influence of sintering aids on silicon carbide microstructure

SEM observations, performed on the three samples NMK-A500, NMK-AY500 and NMK-NA500, are reported in Figure 3. These pictures show a very low level of porosity, mainly located at triple points, for the NMK-A500 and NMK-AY500 samples, consistent with the high measured densities (98-99%). Moreover, Figure 3(b) clearly indicates the presence of secondary phase at grain boundaries and triple points (in white on the image), that corresponds to residual liquid phase. This observation testifies to the mechanism of liquid-phase sintering with the presence of the chosen sintering aids, at least for this sample. This observation is relevant with the sintering behaviour of this sample (Figure 1), which presents a faster sintering kinetic and a beginning of sintering at the lowest temperature.

On its side, the NMK-NA500 sample exhibits porous surface (Figure 3(c)) which is certainly due to removal of superficial grains during polishing. This should explain the difference between SEM surface observation and the high density measured previously. Note that geometrical density measurement was performed on this sample and the result was consistent with the Archimede's density value previously given, giving trust to the hypothesis of surface grain detachment.

Finally, it is possible to observe some twins on most of the grains of each sample. These twins indicate the presence of defects in the crystalline structure of the sintered pellets.

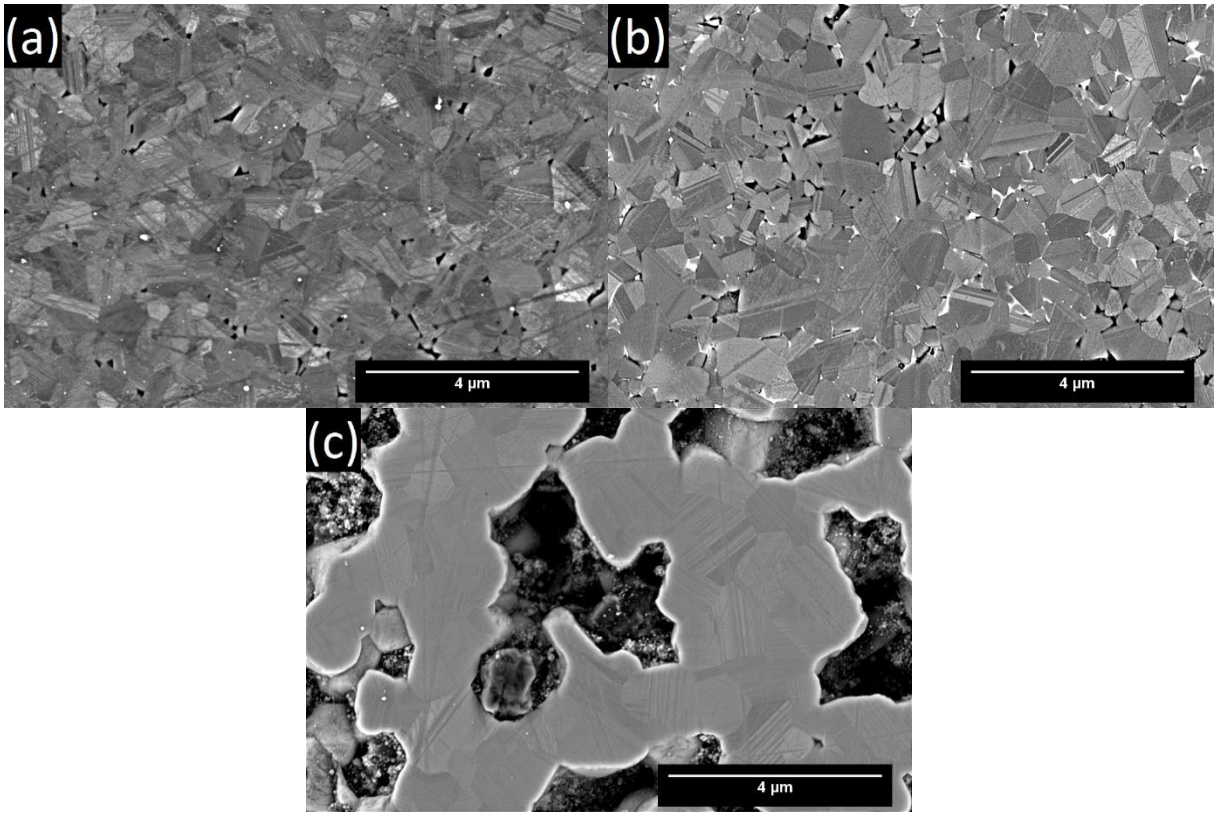

Figure 3 - SEM image obtained from observations of the samples (a) NMK-A500, (b) NMK-AY500 and (c) NMK-NA500

Table 3 reports grain sizes measurements performed on the sintered pellets. All the samples present large grain size distribution and equiaxed grains. The two samples NMK-A500 and NMK-AY500 (Figure 3(a) and Figure 3(b)) show similar grains size, in the range [610-660nm]. These grain sizes are higher than the ones measured on pure SiC samples (320nm for samples with densities of 95% [10], [26]). The difference could come from grains coalescence at the end of the densification, as generally observed during liquid-phase sintering, but also from the low sintering pressure applied that does not limit the driving forces of growth mechanisms [27], [28]. In spite of a majority of equiaxed grains, these two samples (NMK-A500 and NMK-AY500) present few elongated grains, testifying to the presence of the hexagonal crystalline structure [21], [29] due to the high sintering temperature and low pressure. The sample NMK-NA500 (Figure 3(c)) presents a slightly coarser grain size (about 1µm). This could be explained by the appearance of another

sintering mechanism favouring grain growth rather than densification (surface diffusion for example). It is also possible to notice the absence of elongated grains in this sample. This observation is associated with the addition of AlN compound, which is generally recognized in the literature to stabilize the equiaxed shape of grain by inhibition of grain growth [23]–[25].

Table 3 - Summarized table of grain sizes of samples NMK-A500, NMK-AY500 and NMK-NA500

Sample	Grain size (nm)	Standard deviation (nm)
NMK-A500	660	± 220
NMK-AY500	610	± 210
NMK-NA500	990	± 260

This first series of experiments highlight the efficiency of selected sintering aids according to the significant increase in the density of sintered SiC samples, even under low sintering pressure (17MPa) and relatively low temperature. We demonstrated however in a recent study that the application of high sintering pressure could allow increasing the density of sintered pellets while delaying the polytypic transition to higher temperature [10]. These observations let suppose that an increase of sintering pressure could help to compensate a reduced content of sintering aids in order to limit the introduction/formation of secondary phases while developing cubic SiC with density close to 100% of T.D..

Moreover, all these observations showed that a liquid-phase sintering allows obtaining samples with density close to 100%, even under low pressure and low amount of sintering aids (5wt.%). Nevertheless, the microstructure of the sintered pellets reveals a non-negligible grain growth when compared to a ceramic sintered without aids.

3.3 Optimization of the sintering aids content according to the applied pressure

In the following of the study, the decrease of the sintering aid content is investigated while the applied pressure during sintering is increased. The objective is to reduce as much as possible the sintering aid content to limit secondary phases presence and grain growth while maintaining high level of densification and if possible 100% cubic phase.

3.3.1 Influence of sintering aid content

The first studied parameter was the sintering aid content. For that, several tests were performed using 0.5wt. % of sintering aid.

Figure 4 presents SPS curves obtained from sintering experiments and compared with the ones of previous samples (with 5wt.% additives content). These curves show similar dilatation step for all samples. However, it is possible to notice a difference regarding the sintering kinetic during the shrinkage step. Indeed, a lower additive content induces a lower kinetic. Similarly, the total displacement of each sample is much lower (by a factor of 2) when the additive content is lower. These results suggest lower density for samples sintered with lower sintering aid content.

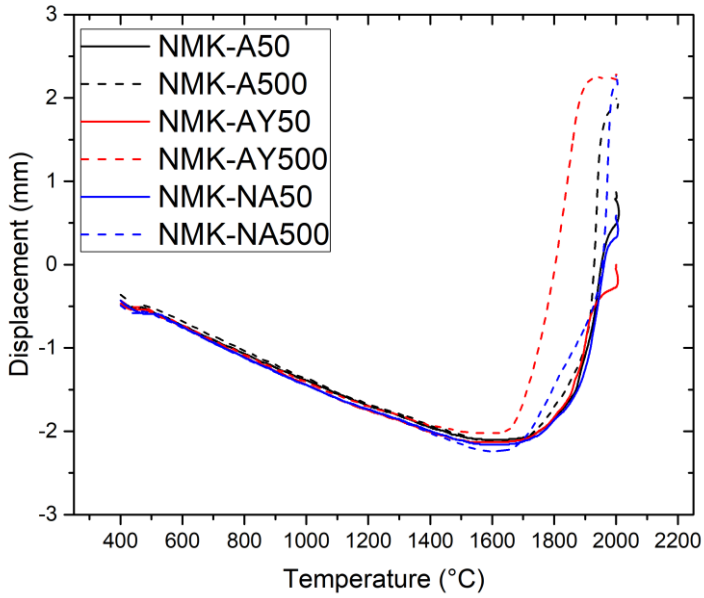

Figure 4 - Sintering behaviour curves of the samples sintered with the 0.5wt% and 5wt% Al_2O_3, Al_2O_3-Y_2O_3 and Al_2O_3-AlN sintering aid

While the three sintered pellets NMK-A500, NMK-AY500 and NMK-NA500 present similar shrinkage, the others show a different behaviour. Indeed, it is possible to notice displacement values of 0.3mm, 0.9mm and 1.2mm respectively for the samples NMK-AY50, NMK-NA50 and NMK-A50. These results seem to indicate differences regarding the density of these pellets. Indeed, Archimede's densities measurements (Table 4) confirm these results: sample NMK-AY50, presenting lower shrinkage, has a density of 72% while the sintered pellet NMK-A50, presenting higher shrinkage, reaches a density of 80%.

Nevertheless, this table shows an exception: despite a much lower shrinkage (0.9mm compared to 2.5mm), the sample NMK-NA50 presents the same density than the sample NMK-NA500. This observation shows that Al_2O_3-AlN strongly influence the densification behaviour of SiC even with low content addition.

These results also show that a decrease of sintering aid content leads to the decrease of the final relative density for samples sintered in the same conditions. The addition of low content of sintering aid still allows improving of about 20-30% the density of the compact, according to the nature of the dopant, compared to the one obtained after the sintering of raw NMK.

Table 4 - Summarized table presenting densities of the samples sintered with the Al_2O_3, Al_2O_3-Y_2O_3 and Al_2O_3-AlN mixtures and different contents

Sample	Density (% of T.D.)
NMK-A50	80 ± 1%
NMK-A500	99 ± 1%
NMK-AY50	72 ± 1%
NMK-AY500	99 ± 1%
NMK-NA50	99 ± 1%
NMK-NA500	98 ± 1%

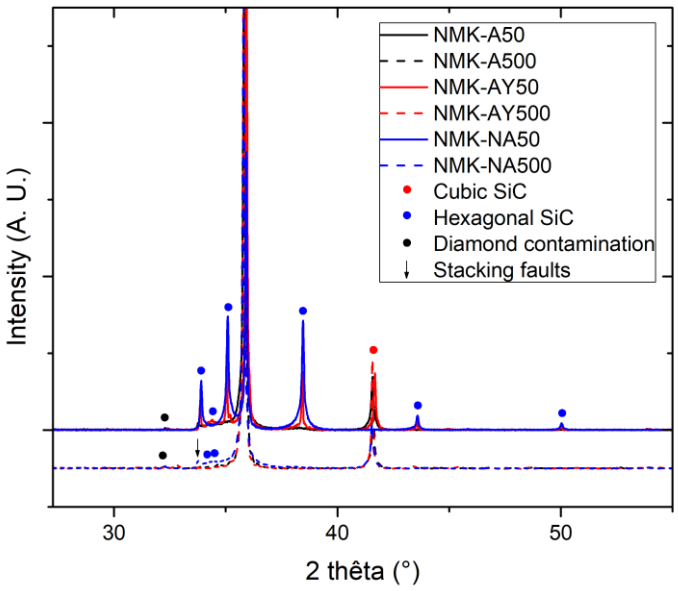

Figure 5 - Experimental XRD patterns of the samples sintered with the Al_2O_3, Al_2O_3-Y_2O_3 and Al_2O_3-AlN mixtures and different contents

XRD analyses were performed on the latter samples. Experimental XRD patterns obtained were reported in Figure 5. No sample presents only a pristine cubic crystalline structure. Indeed, the high temperatures applied (2000°C), combined with the low pressure (17MPa), makes the polytypic transformation of SiC foreseeable. While samples with aid contents of 5wt.% only present the 3C and 6H polytypes of SiC, it is possible to observe other Bragg peaks for samples NMK-AY50 and NMK-NA50. These peaks are respectively identified at 2θ = 33.8°, 34.8°, 38.3°, 43.4° and 49.9° and are attributed to the 4H polytype of SiC (JCPDS card 01-072-4532). The presence of this crystalline structure in the sample NMK-AY50 certainly comes from the presence of intermediary states which could appear during the 3C-6H transition, as reported in the literature by Sugiyama and Togaya [30]. Its presence in the sample NMK-NA50 could come from either the same kind of intermediary state during the polytypic transition [30] or the presence of pure aluminium, which could favour the 3C-4H transition during sintering at high temperature as reported by Jepps and Page [31]. Indeed, it could be possible, in this case, that a low content of free-Al was introduced during the addition of Al_2O_3-AlN. The high temperature and the low applied pressure could then allow this polytypic transformation, despite the presence of nitrogen in the sample NMK-NA50, generally reported as stabilizing the cubic phase [17], [23]–[25]. Then, it is possible to identify the presence of the (101) atomic plane of the 6H polytype at 2θ = 34.2° [32] in the experimental XRD patterns of the samples NMK-AY50 and NMK-A50.

The presence of sintering aids or secondary phases has not been highlighted in these experimental XRD patterns. Indeed, the low content (0.5wt.%) can be considered as lower than the detection threshold of the XRD apparatus, generally considered at about 1%. These 6 samples also present a characteristic peak, identified at $2\theta = 32°$, attributed to a above mentioned carbon contamination.

These results indicate that it is possible to obtain relatively high densities (72% and 80% of T.D.), even with low content of sintering additives. It is even possible to reach the maximal density (99%) with the addition of Al_2O_3-AlN mixture. Nevertheless, the applied pressure during sintering is too low to avoid polytypic transformations in the SiC pellets. Applying higher pressure could allow to improve and/or maintain the density of sintered pellets while limiting the formation of other polytypes.

3.3.2 Influence of applied pressure

In order to evaluate the influence of pressure on the density and the crystalline structure of the sintered samples additional SPS experiments were performed under higher pressures. Note that we fixed here the sintering aids contents to 0.5wt.% to limit the presence of secondary phases. However, the application of higher sintering pressure is expected to increase samples final density, as recently published in our previous work [10].

SPS testing were carried out under two pressures, respectively 80MPa and 127MPa (progressively applied from 1160°C up to 1200°C), with a heating rate of 10°C/min up to 2000°C and a dwell of 10 minutes at maximal temperature. Sintering curves are reported in Figure 6 and compared with the ones obtained for experiments under lower pressure (17MPa).

All these curves show a similar dilatation for each sample during the heating step. The sintering kinetic of 80MPa-sintered samples seems similar whatever the added sintering aid. These samples also present equivalent shrinkage, supposing densities in the same order of magnitude.

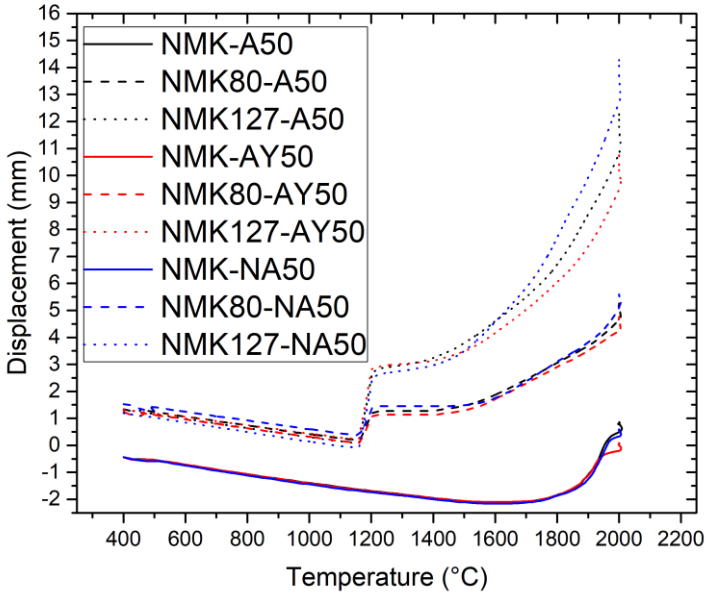

Figure 6 - Sintering behaviour curves of the samples sintered with the Al_2O_3, Al_2O_3-Y_2O_3 and Al_2O_3-AlN mixtures with content of 0.5wt.% under different sintering pressures

The samples sintered under high pressure (127MPa) present slightly different sintering kinetic and final shrinkage. Indeed, it seems that the Al_2O_3-Y_2O_3 bearing mixture is the less efficient, while the Al_2O_3-AlN one presents a faster kinetic and higher shrinkage. Nevertheless, the density measurements (Table 5) reveal no difference between the different samples, despite the gap in the overall shrinkage. Relative densities of about 98-99% are indeed obtained for pressure equal or higher than 80MPa. The difference of displacement can be explained by elastic and/or plastic deformation of the sintering tools under high pressure and high temperature [33].

Table 5 - Densities of sintered samples with the Al_2O_3, Al_2O_3-Y_2O_3 and Al_2O_3-AlN mixtures with content of 0.5wt.% under different pressures

Sample	Density (% of T.D.)
NMK-A50	80 ± 1%
NMK80-A50	99 ± 1%
NMK127-A50	99 ± 1%
NMK-AY50	72 ± 1%
NMK80-AY50	98 ± 1%

NMK127-AY50	99 ± 1%
NMK-NA50	99 ± 1%
NMK80-NA50	98 ± 1%
NMK127-NA50	99 ± 1%

Experimental XRD patterns of samples sintered under different pressures are reported in Figure 7. These results show that, in addition to the huge increase of density, the application of a high pressure during sintering leads to stabilize the cubic structure of SiC and thus to shift the polytypic transition towards higher temperature. Indeed, some Bragg peaks of the 6H polytype are noticed in the experimental patterns of 80MPa-sintered samples, while the 127MPa-sintered samples only show those of the cubic structure. These results are consistent with the ones obtained during the sintering of the raw NMK [10]. Moreover, the Bragg peak indicating the presence of 4H polytype also disappeared for pressures equal or higher than 80MPa.

In this case, no peak linked to the presence of secondary phases is noticed. Sintering aids contents indeed remain lower than the detection threshold of the XRD apparatus.

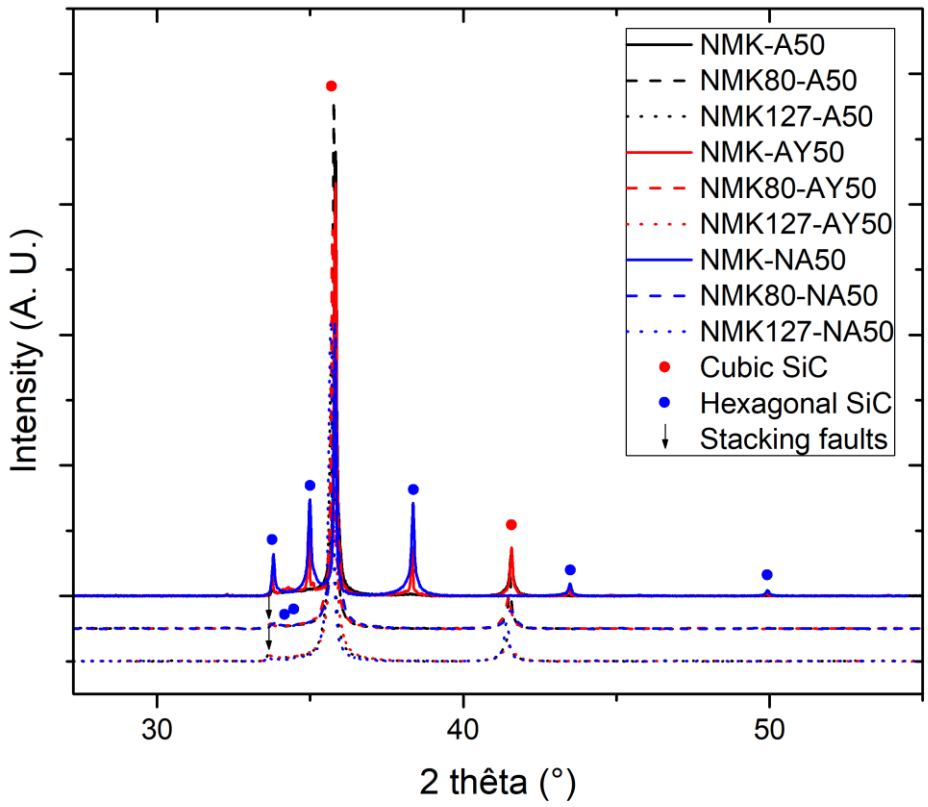

Figure 7 - Experimental XRD patterns of samples sintered with the Al_2O_3, Al_2O_3-Y_2O_3 and Al_2O_3-AlN mixtures with content of 0.5wt.% under different pressures

3.3.3 Microstructural observations

Microstructural observations were performed on samples sintered under 80MPa and 127MPa with addition of 0.5wt.% of sintering aids. Figure 8 shows images obtained from samples sintered under 80 MPa. These observations indicate a very low porosity related to the high density of the samples (98-99%). Note that geometrical density measurements were performed on these samples and the results were consistent with the Archimede's density values previously given.

Figure 8(a) shows that the sample NMK80-A50 presents a majority of equiaxed grains. The presence of few elongated grains testifies to the presence of the 6H polytype in the crystalline structure of this sample [21], [29]. The grain size measurements (Table 6) indicates a microstructure slightly smaller (610nm against 660nm) than the one obtained with a sintering experiment under 17MPa and an addition of 5wt.% of alumina as dopant. This observation indicates that applying pressure allows to reduce the dopant content while

keeping high density and finally could limit the phenomenon of growth at the end of densification. Nevertheless, this sample presents a grain size much larger than the one measured on samples sintered with the raw powder, i.e., 500nm for a free-additive sample sintered under 80MPa at a temperature of 2000°C.

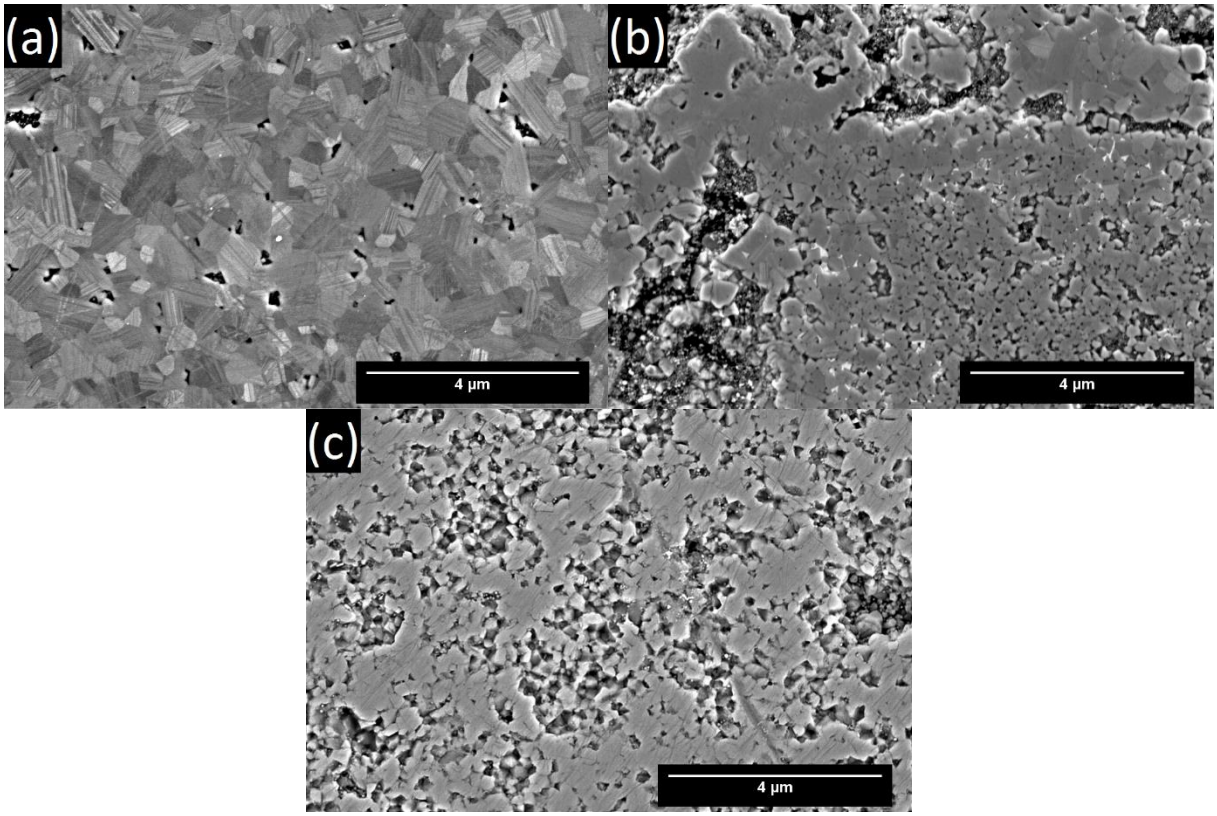

Figure 8 - SEM images obtained from observations on the samples (a) NMK80-A50, (b) NMK80-AY50 and (c) NMK80-NA50

Table 6 - Summarized table of grain sizes of samples NMK80-A50, NMK80-AY50 and NMK80-NA50

Sample	Grain size (nm)	Standard deviation
NMK80-A50	610	± 180
NMK80-AY50	320	± 130
NMK80-NA50	290	± 80

At the opposite, the two samples NMK80-AY50 and NMK80-NA50 (Figure 8(b) and (c)) present smaller grain sizes than the one obtained with the sintering of raw powder (about 500nm). This observation indicates that in this case, the grain growth is limited by applying sintering pressure and a decrease of sintering aids content. It is possible to suppose that the addition of pure alumina could favour both grain growth and densifying mechanisms, contrary to the addition of Al_2O_3-Y_2O_3 and Al_2O_3-AlN compounds, which certainly favour only the densifying mechanisms. These two samples also present homogeneous microstructure with equiaxed grains. The superficial porosity observed in Figure 8(b) and (c) certainly comes from either removal of superficial grains during polishing or low-dense superficial layer due to the surface contamination by graphite environment during SPS.

The observation of these three samples does not allow noticing the presence of liquid residual phases in the porosity. Indeed, the low added content limits the formation of liquid phase and secondary phases.

Finally, each sample presents some twins in its microstructure, in line with the presence of defects in the crystalline structure.

Other observations were performed on samples sintered under 127MPa with 0.5wt.% of dopants. The obtained images were reported in Figure 9 and the grain size measurements in Table 7. Note that geometrical density measurements were also performed on these samples and the results were consistent with the Archimede’s density values previously given.

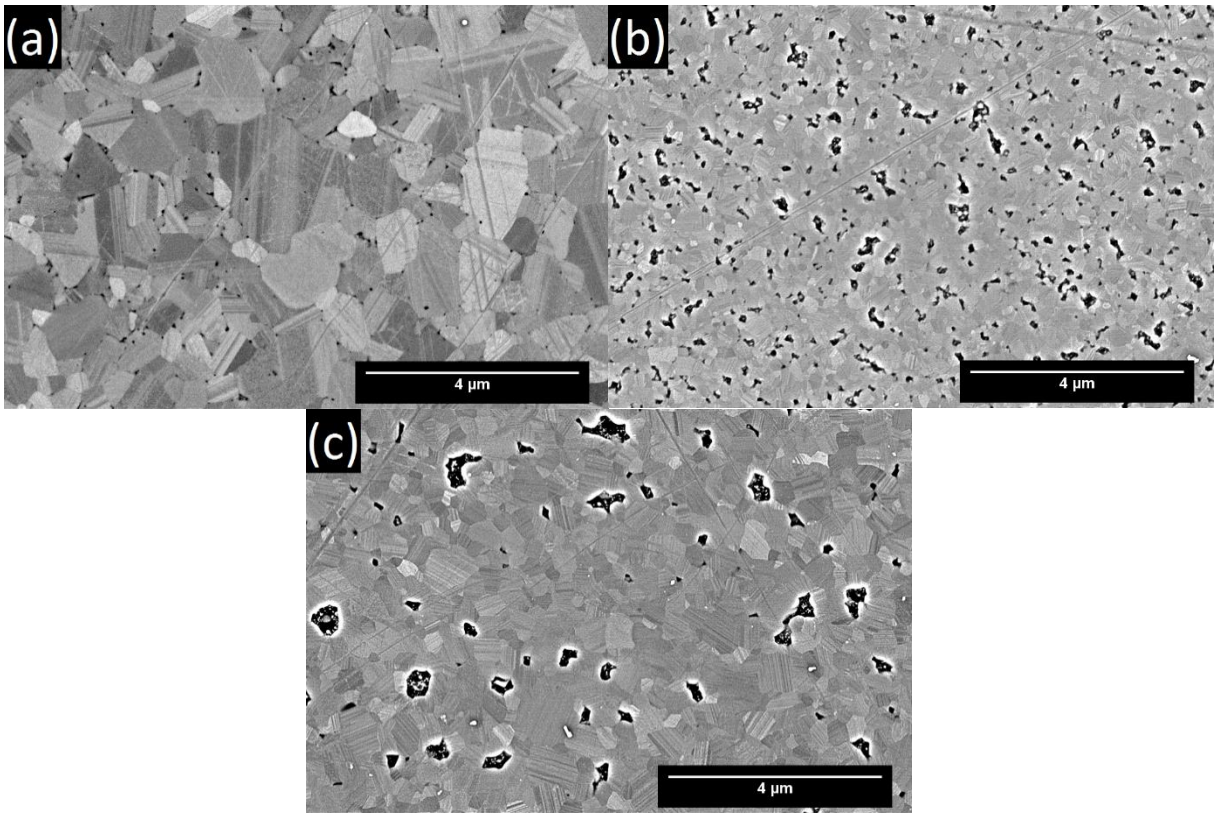

Figure 9 - SEM images obtained from observations of the samples (a) NMK127-A50, (b) NMK127-AY50 and (c) NMK127-NA50

Table 7 - Summarized table of grain sizes of samples NMK127-A50, NMK127-AY50 and NMK127-NA50

Sample	Grain size (nm)	Standard deviation
NMK127-A50	1630 650	± 350 ± 200
NMK127-AY50	270	± 60
NMK127-NA50	500	± 190

These images show that the microstructure of the sample NMK127-A50 differs from the two other samples. Indeed, despite the application of very high sintering pressure, it is possible to observe an abnormal grain growth. Two population of grains appear, respectively of about 1.6µm and 650nm. The microstructure shows different shapes of grains. It is also possible to observe the presence of twins on each grain of this sample.

The two other samples present a similar microstructure than the one observed previously. The SEM image on Figure 9(b) indicates that the sample NMK127-AY50 presents perfectly

equiaxed grains with fine microstructure, lower than 300nm. The sample NMK127-NA50 (SEM image Figure 9(c)) also presents perfectly equiaxed grains. Nevertheless, it shows a microstructure with larger average grains size of about 500nm, testifying to the coalescence phenomena at the end of densification despite the high applied pressure. These two samples also present structural defects (twins).

These different observations show that it is possible to obtain samples with fine and homogeneous microstructure and very low porosity, even with low content of added sintering aids. These microstructures are expected to induce high mechanical performance.

4 Conclusion

The influence of the addition of dopants on the densification behaviour, microstructure, crystalline structure, and density of spark plasma sintered SiC pellets was studied in this paper.

We have highlighted the strong influence of three sintering aids (Al_2O_3, Al_2O_3-Y_2O_3 and Al_2O_3-AlN) on the densification rate of SiC. Indeed, we firstly demonstrated the possibility to develop SiC samples with high density (99%) with only 5wt.% of dopants. However, we noticed the presence of 6H, even 4H, polytypes in these samples, due to the low applied pressure (17MPa) and the high sintering temperature (2000°C). The application of high sintering pressure (127MPa) allowed us to keep the pristine cubic crystalline structure of our samples while strongly reducing the dopants content down to 0.5wt.% and thus limiting the presence of impurities and secondary phases.

The SEM observations of sintered samples revealed microstructure consisting of equiaxed grains, with average sizes of 300nm and 500nm respectively for Al_2O_3-Y_2O_3 and Al_2O_3-AlN dopants.

Finally, we showed the possibility to develop cubic SiC samples with high density (99%) and fine microstructure with only a very low content of sintering aids (0.5wt.%).

5 Acknowledgements

F. Delobel is now working as researcher in the Belgian Ceramic Research Centre (Mons).

The authors thank the ISL (French-German Research Institute of Saint-Louis) for funding on silicon carbide ceramics development.

6 References

[1] R. Riedel, Ed., *Handbook of Ceramic Hard Materials*. Weinheim, Germany: Wiley-VCH Verlag GmbH, 2000. doi: 10.1002/9783527618217.

[2] J. W. McCauley, 'Ceramic armor materials by design: proceedings of the Ceramic Armor Materials by Design Symposium', presented at the Pac Rim IV International Conference on Advanced Ceramics and Glass, Wailea, Maui, Hawaii, 2002. Accessed: Apr. 03, 2019. [Online]. Available: http://search.ebscohost.com/login.aspx?direct=true&scope=site&db=nlebk&db=nlabk&AN=1463042

[3] R. E. Tressler, 'An assessment of low cost manufacturing technology for advanced structural ceramics and its impact on ceramic armor', in *Ceramic Armor Materials by Design*, Westerville, Ohio: The American Ceramic Society, 2001, pp. 451–462.

[4] M. Chen, 'Shock-Induced Localized Amorphization in Boron Carbide', *Science*, vol. 299, no. 5612, pp. 1563–1566, Mar. 2003, doi: 10.1126/science.1080819.

[5] *Silicon Carbide–1968*. Elsevier, 1969. doi: 10.1016/C2013-0-01599-X.

[6] V. V. Pujar, R. P. Jensen, and N. P. Padture, 'Densification of liquid-phase-sintered silicon carbide', *Journal of Materials Science Letters*, vol. 19, no. 11, pp. 1011–1014, 2000, doi: 10.1023/A:1006753213286.

[7] Y.-W. Kim, M. Mitomo, and G.-D. Zhan, 'Mechanism of grain growth in liquid-phase-sintered β–SiC', *Journal of Materials Research*, vol. 14, no. 11, pp. 4291–4293, Nov. 1999, doi: 10.1557/JMR.1999.0581.

[8] A. Kaiser, R. Vassen, D. Stöver, and H. P. Buchkremer, 'Heat treatment of ultrafine SiC powders to reduce oxidation sensitivity and grain growth', *Nanostructured Materials*, vol. 4, no. 7, pp. 795–802, Jan. 1994, doi: 10.1016/0965-9773(94)90085-X.

[9] S. Lemonnier *et al.*, 'Multimodal particle size distribution by mixing nanopowders for full densification of spark plasma sintered SiC ceramics', *Open Ceramics*, vol. 7, p. 100164, Sep. 2021, doi: 10.1016/j.oceram.2021.100164.

[10] F. Delobel, S. Lemonnier, É. Barraud, and J. Cambedouzou, 'Influence of sintering temperature and pressure on the 3C-6H transition of silicon carbide', *Journal of the European Ceramic Society*, vol. 39, no. 2–3, pp. 150–156, Feb. 2019, doi: 10.1016/j.jeurceramsoc.2018.09.010.

[11] D. Bernache-Assollant and J.-P. Bonnet, 'Frittage: aspects physico-chimiques Partie 2: frittage en phase liquide', *Techniques de l'ingénieur. Sciences fondamentales*, no. AF6621, p. AF6621. 1-AF6621. 14, 2005.

[12] F. F. Lange, 'Hot-pressing behaviour of silicon carbide powders with additions of aluminium oxide', *Journal of Materials Science*, vol. 10, no. 2, pp. 314–320, 1975, doi: 10.1007/BF00540356.

[13] M. D. Unlu, G. Goller, O. Yucel, and F. C. Sahin, 'The Spark Plasma Sintering of Silicon Carbide Ceramics Using Alumina', *Acta Physica Polonica A*, vol. 125, no. 2, pp. 257–259, 2014.

[14] J.-Y. Kim, Y.-W. Kim, J.-G. Lee, and K.-S. Cho, 'Effect of annealing on mechanical properties of self-reinforced alpha-silicon carbide', *Journal of Materials Science*, vol. 34, no. 10, pp. 2325–2330, 1999, doi: 10.1023/A:1004585910170.

[15] H. K. Yoon, Y. J. Lee, H. J. Cho, and T. G. Kim, 'A study on the role of sintering additives for fabrication of SiC ceramic', *International Journal of Modern Physics B*, vol. 24, no. 15n16, pp. 2928–2933, 2010, doi: 10.1142/S0217979210065878.

[16] H. Xu, T. Bhatia, A. Deshpande Swarnima, P. Padture Nitin, L. Ortiz Angel, and L. Cumbrera Francisco, 'Microstructural Evolution in Liquid-Phase-Sintered SiC: Part I, Effect of Starting Powder', *Journal of the American Ceramic Society*, vol. 84, no. 7, pp. 1578–1584, 2001, doi: 10.1111/j.1151-2916.2001.tb00880.x.
[17] K. Strecker, S. Ribeiro, D. Camargo, R. Silva, J. Vieira, and F. Oliveira, 'Liquid phase sintering of silicon carbide with AlN/Y2O3, Al2O3/Y2O3 and SiO2/Y2O3 additions', *Materials Research*, vol. 2, pp. 249–254, 1999.
[18] S. Sigl Lorenz and H.-J. Kleebe, 'Core/Rim Structure of Liquid-Phase-Sintered Silicon Carbide', *Journal of the American Ceramic Society*, vol. 76, no. 3, pp. 773–776, 1993, doi: 10.1111/j.1151-2916.1993.tb03677.x.
[19] A. Deshpande Swarnima, T. Bhatia, H. Xu, P. Padture Nitin, L. Ortiz Angel, and L. Cumbrera Francisco, 'Microstructural Evolution in Liquid-Phase-Sintered SiC: Part II, Effects of Planar Defects and Seeds in the Starting Powder', *Journal of the American Ceramic Society*, vol. 84, no. 7, pp. 1585–1590, 2004, doi: 10.1111/j.1151-2916.2001.tb00881.x.
[20] Y.-W. Kim, M. Mitomo, and H. Hirotsuru, 'Microstructural Development of Silicon Carbide Containing Large Seed Grains', *Journal of the American Ceramic Society*, vol. 80, no. 1, pp. 99–105, 1997, doi: 10.1111/j.1151-2916.1997.tb02796.x.
[21] G.-D. Zhan, R.-J. Xie, M. Mitomo, and Y.-W. Kim, 'Effect of β-to-α Phase Transformation on the Microstructural Development and Mechanical Properties of Fine-Grained Silicon Carbide Ceramics', *Journal of the American Ceramic Society*, vol. 84, no. 5, pp. 945–950, 2001, doi: 10.1111/j.1151-2916.2001.tb00773.x.
[22] P. T. B. Shaffer, 'Beta Silicon Carbide', in *Silicon Carbide-1968*, Pergamon, 1969, pp. S97–S105. doi: 10.1016/B978-0-08-006768-1.50014-0.
[23] K. Suzuki and M. Sasaki, 'Microstructure and mechanical properties of liquid-phase-sintered SiC with AlN and Y2O3 additions', *Ceramics International*, vol. 31, no. 5, pp. 749–755, 2005.
[24] A. L. Ortiz, T. Bhatia, N. P. Padture, and G. Pezzotti, 'Microstructural Evolution in Liquid-Phase-Sintered SiC: Part III, Effect of Nitrogen-Gas Sintering Atmosphere', *Journal of the American Ceramic Society*, vol. 85, no. 7, pp. 1835–1840, 2002, doi: 10.1111/j.1151-2916.2002.tb00361.x.
[25] K. Raju and D.-H. Yoon, 'Sintering additives for SiC based on the reactivity: A review', *Ceramics International*, vol. 42, no. 16, pp. 17947–17962, 2016, doi: https://doi.org/10.1016/j.ceramint.2016.09.022.
[26] F. Delobel, S. Lemonnier, R. D'Elia, and J. Cambedouzou, 'Effects of density on the mechanical properties of spark plasma sintered β-SiC', *Ceramics International*, vol. 46, no. 9, pp. 13244–13254, Jun. 2020, doi: 10.1016/j.ceramint.2020.02.101.
[27] Z. Guo-Dong, I. Yuichi, M. Mamoru, X. Rong-Jun, S. Taketo, and M. A. K, 'Microstructural Analysis of Liquid-Phase-Sintered β-Silicon Carbide', *Journal of the American Ceramic Society*, vol. 85, no. 2, pp. 430–436, 2002, doi: 10.1111/j.1151-2916.2002.tb00107.x.
[28] R. M. German, P. Suri, and S. J. Park, 'Review: liquid phase sintering', *Journal of Materials Science*, vol. 44, no. 1, pp. 1–39, 2009, doi: 10.1007/s10853-008-3008-0.
[29] G.-D. Zhan, M. Mitomo, H. Tanaka, and Y.-W. Kim, 'Effect of Annealing Conditions on Microstructural Development and Phase Transformation in Silicon Carbide', *Journal of the American Ceramic Society*, vol. 83, no. 6, pp. 1369–1374, 2000, doi: 10.1111/j.1151-2916.2000.tb01395.x.
[30] S. Sugiyama and M. Togaya, 'Phase Relationship between 3C- and 6H-Silicon Carbide at High Pressure and High Temperature', *Journal of the American Ceramic Society*, vol. 84, no. 12, pp. 3013–3016, Dec. 2001, doi: 10.1111/j.1151-2916.2001.tb01129.x.
[31] N. W. Jepps and T. F. Page, 'Polytypic transformations in silicon carbide', *Progress in Crystal Growth and Characterization*, vol. 7, no. 1–4, pp. 259–307, Jan. 1983, doi: 10.1016/0146-3535(83)90034-5.
[32] V. V. Pujar and J. D. Cawley, 'Effects of Stacking Faults on the X-ray Diffraction profiles of β-SiC powders', *Journal of American Ceramic Society*, vol. 774, p. 82, 1995.

[33] C. Manière, G. Lee, J. McKittrick, A. Maximenko, and E. A. Olevsky, ‘Graphite creep negation during flash spark plasma sintering under temperatures close to 2000 °C’, *Carbon*, vol. 162, pp. 106–113, Jun. 2020, doi: 10.1016/j.carbon.2020.02.027.